Thermochimica Acta, 205 (1992) 191–203
Elsevier Science Publishers B.V., Amsterdam

Gibbsite; XRD; DTA; Crystallinity; Transformation, Aluminium hydroxide; Boehmite;

A new approach to phase transformations in gibbsite: the role of the crystallinity

S.K. Mehta [a], Ashok Kalsotra [a] and M. Murat [b]

[a] *Regional Research Laboratory, Canal Road, Jammu Tawi 180001 (India)*
[b] *Groupe d'Etudes Métallurgie Physique et Physique des Matériaux (GEMPPM, U.R.A. CNRS No. 341), INSA de Lyon, 20 avenue Albert Einstein, 69621 Villeurbanne Cedex (France)*

(Received 30 October 1991)

Abstract

Samples of gibbsite have been classified into well crystallized and poorly crystallized by X-ray and differential thermal analysis methods. The thermal reaction shows that the degree of crystallinity affects the course of the transformation. The electrical conductivity and dielectric measurements show a marked change at the transformation temperatures. The effect of crystallinity on the orientation relations between lattices of different structural phases of gibbsite is discussed.

INTRODUCTION

Gibbsite (natural aluminium trihydrate, $Al(OH)_3$), like boehmite AlOOH and diaspore AlO_2H, is a constituent of bauxites [1]. Synthetic gibbsite is obtained by crystallization from sodium aluminate solution by the Bayer process [2]. Synthetic corundum (or α-alumina) is prepared by calcination in air of pure gibbsite (natural or synthetic). The nature of the phases appearing during the transformation of gibbsite (boehmite and/or more or less amorphous transitory aluminas, including 'gamma', 'delta', 'eta', 'theta', 'kappa', 'chi', etc.) were discussed in many papers in the 50s and 60s [3–5] and more recently summarized [6,7] owing to the interest in these solids as catalyst supports and ceramic raw materials. In the 80s the thermal stability of transitory aluminas was largely investigated because of the interest in these solid phases as catalysts for automotive emission control [8,9].

There are many broad schools of thought regarding the mechanism of the transformations of aluminium hydroxides (and especially gibbsite). These transformations are shown in Fig. 1 [6,7,10].

Correspondence to: M. Murat, Groupe d'Etudes Métallurgie Physique et Physique des Matériaux (GEMPPM, U.R.A. CNRS No. 341) INSA de Lyon, 20 avenue Albert Einstein, 69621 Villeurbanne Cedex, France.

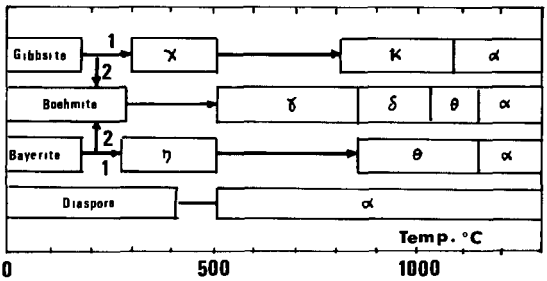

Fig. 1. Dehydration sequence of alumina hydrates in air [6,7]: route 1 is favoured with low grain-size particles; route 2 by humidity, alkalinity and high grain-size particles.

However, the transformation of gibbsite in an autoclave up to about 400°C leads to boehmite, then to α-alumina at higher temperatures [11].

Recent investigations of Burtin and co-workers [9,10] have shown that the transitional γ-, δ-and θ-aluminas obtained by dehydration of boehmite, are solid solutions and can be described by the unique formula

$$Al_2 \square O_{3-\upsilon/2}(OH)_{\upsilon} \langle\ \rangle_{1-\upsilon/2}$$

in which Al represents the aluminium ions in the trivalent sites, $\square$ the cationic vacancies in the divalent sites, OH the hydroxyl groups substituting the oxygen in the normal positions of the anionic sublattice and $\langle\ \rangle$ the anionic vacancies of the spinel structure.

Thus, the formulae of boehmite ($\upsilon = 2$) and α-alumina ($\upsilon = 0$) are $Al_2 \square O_2(OH)_2$ and $Al_2 \square O_3$ respectively.

It is possible that this accurate definition of the chemical formula could be extended to χ- and κ-alumina formed by dehydration of gibbsite.

According to Burtin and co-workers [9,10], the transformations $\gamma \rightarrow \delta \rightarrow \theta$ proceed topotactically in relation to the development of microporosity (the relative intensities of X-ray lines are not modified during the transformations by growth of the new phase in certain preferential crystalline directions).

In the same way, and according to Varhegye et al. [12], in the gibbsite $\rightarrow$ χ-$Al_2O_3 \rightarrow \kappa$-$Al_2O_3 \rightarrow \alpha$-$Al_2O_3$ sequence, the crystalline form of the original gibbsite is retained and the product obtained can be considered a pseudomorph of the initial gibbsite: the growth of corundum crystal proceeds in almost parallel planes on the prism faces of the pseudomorph corresponding to the gibbsite lattice (in the direction [*kki*O]).

The development of advanced ceramics or composites with alumina matrices has led us to start new investigations on the problem of production of α-alumina by the thermal transformation of gibbsite, the objective being to control the morphological and physico-chemical properties of the reaction product in relation to the subsequent sintering of α-alumina ceramic bodies.

The present paper describes some observations on both the role of the crystallinity of gibbsite on the mechanism of transformation and the orientation relationship between the different crystal structures obtained.

SAMPLES INVESTIGATED

Two types of synthetic gibbsite samples were investigated: a Bayer's alumina sample and synthetic samples grown in the laboratory by precipitating aluminium as aluminium hydroxide [13]

$$AlCl_3 + 3NH_4OH \rightarrow Al(OH)_3 + 3NH_4Cl$$

Ammonium hydroxide was added dropwise to a solution of aluminium chloride in order to avoid the abrupt precipitation of aluminium hydroxide. Methyl orange was used as an indicator. Further addition of ammonium was stopped when the colour of the indicator vanished. The precipitates thus obtained were filtered and washed with excess water until the filtrate did not react positively to the test for chloride ion. The $Al(OH)_3$ was dried in an electric oven at 100°C and the dried mass was crushed and sieved through 200 B.S.S. mesh.

The X-ray analysis of the two types of sample revealed that the Bayer's alumina was highly crystalline and that the alumnium trihydrate grown in the laboratory was poorly crystalline.

In the X-ray diffractograms of the highly crystalline samples (Fig. 2, curve a), the X-ray lines (interplanar spacing) are large in number and the

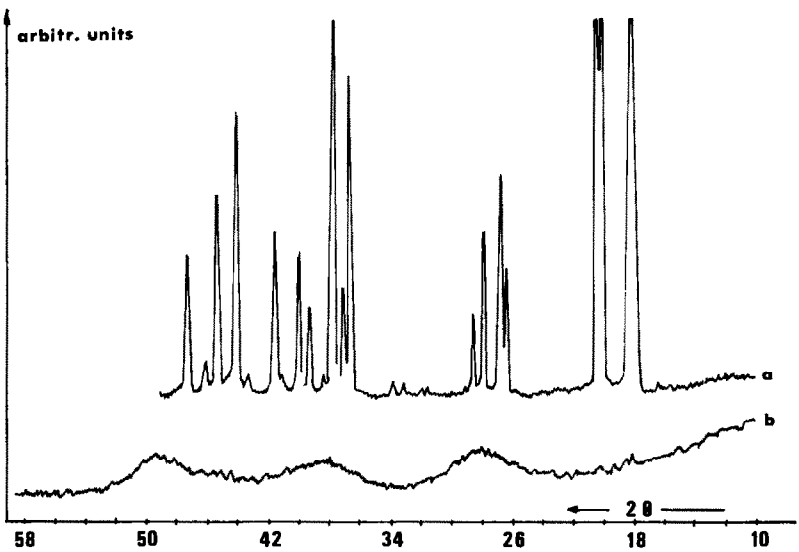

Fig. 2. X-ray powder diffractogram of a well crystallized sample (curve a); and a poorly crystallized sample (curve b).

TABLE 1

Crystal size for the well crystallized gibbsite sample

hkl	2θ (deg)	$\beta 1/2$	Dhkl (Å)
002	18.4	0.067	1201
313	44.22	0.069	1207
024	52.22	0.069	1282

closely spaced lines are well resolved. In the poorly crystalline samples (Fig. 2, curve b), the lines are fewer in number and the closely spaced lines are broad and diffuse bands; the intensity of the reflections as a function of $\sin(\theta/\lambda)$ is much reduced, indicating that some sort of lattice disorder has resulted from the unfavorable conditions of gibbsite crystallization.

The crystallite size of the highly crystalline samples was determined at room temperature using the Scherrer equation; results are given in Table 1.

The X-ray diffraction peaks of the poorly crystallized sample were very broad and thus crystallite size measurements were not possible. The line broadening technique shows that when crystallite size decreases to a certain limit, the crystallites essentially allow the X-ray beam to diverge as it leaves, because the diffracting planes are no longer infinite in length compared with the incident wavelength. This measurement of crystallite size revealed that the poorly crystalline samples have a very small crystallite size, almost equal to the incident wavelength (a few Ångstroms).

EXPERIMENTAL

To study the thermal transformations, the samples of gibbsite were heated in air in an electric furnace with a temperature variation of ± 5°C.

The transformation of gibbsite into α-alumina was investigated using the following experimental methods.

(i) X-ray analysis of the sample was carried out using a Phillips X-ray powder diffractometer (PW 1350), operated at 30 kV and 10 mA using Cu Kα radiation, with a scanning speed of 1 Å in 2θ per minute.

(ii) Thermal analysis: TG and DTA analysis were carried out on a MOM Derivatograph (Budapest, Hungary) at a linear heating rate of 10°C min^{-1}, with α-alumina as internal standard.

(iii) For the electrical conductivity measurements, samples of gibbsite powder were compacted at 12000 psi in a hydraulic press (Carver laboratory press, USA) at room temperature using stainless steel moulds. The flat surface of the pellets were made conducting by coating aquadag paint on both the surfaces. The coated samples were placed on the platform of the lower electrode on the sample holder [14]. This sample holder is fitted with a heating coil. The resistance of the sample was measured after every 20°C

interval using a Million Meg-ohmeter RM 160 MKIII at a constant test voltage. The values of the resistance below the megaohm range (less than 10^6 Ω) were measured using a P-Phillips voltmeter. The specific resistance was calculated, the reciprocal of which gave the electrical conductivity. The temperature of the specimen was allowed to rise slowly at a constant rate of 10°C min^{-1}. The temperature of the sample was measured by a chromel–alumel thermocouple inserted in the sample holder which just touched the side of the specimen.

(iv) For the experimental determination of the dielectric constant, the Heterodyne Beat method [15] was used. This method depends on an adjustment of the test condenser and calibrated variable condenser to the same total capacity, with and without the sample. The test samples are in the form of solid discs. Solid discs of samples preheated [16] from 100 to 970°C were prepared at a dead load of 12000 psi in a hydraulic press (as used in the electrical conductivity measurements). The dielectric constant values of the pellets at a fixed frequency (5000 kHz) were measured and plotted against temperature.

RESULTS AND DISCUSSION

DTA and X-ray diffraction results

The thermal transformation of gibbsite in air differs with the degree of crystallinity, which suggests that the thermal reaction may be due to the presence of defects such as dislocations, grains, boundaries, etc., in the crystal. It is well known that in poorly crystallized materals, these defects are greater in number than in well crystallized materials.

Thus, the following two schemes can be proposed. With well crystallized samples inside the core of the sample

$$\text{Gibbsite} \xrightarrow{300°C} \text{boehmite} \xrightarrow{550°C} \gamma\text{-}Al_2O_3 \xrightarrow{850°C} \theta\text{-}Al_2O_3 \xrightarrow{1000°C} \alpha\text{-}Al_2O_3$$

at the outer periphery of the sample

$$\text{Gibbsite} \xrightarrow{300°C} \chi\text{-}Al_2O_3 \xrightarrow{800°C} \kappa\text{-}Al_2O_3 \xrightarrow{1100°C} \alpha\text{-}Al_2O_3$$

With poorly crystallized samples

$$\text{Gibbsite (P.Cr.)} \xrightarrow{300°C} \chi\text{-}Al_2O_3 \xrightarrow{850°C} \kappa\text{-}Al_2O_3 \xrightarrow{1100°C} \alpha\text{-}Al_2O_3$$

For the poorly crystallized sample, it is seen from the DTA thermograms (Fig. 3) that a single main endotherm is observed in the vicinity of 300°C, while well crystallized samples have a doublet. The doublet is due to the transformation of gibbsite to boehmite and χ-alumina while the single main endotherm in poorly crystallized gibbsite is due to the transformation of gibbsite to χ-Al_2O_3 only.

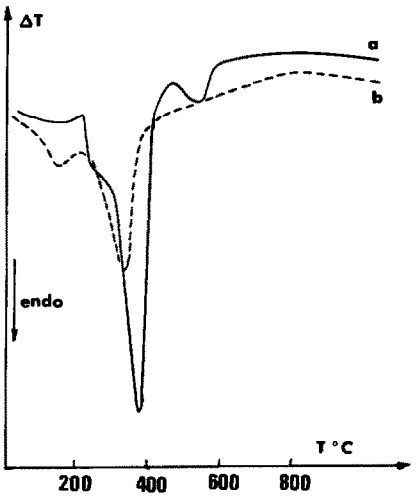

Fig. 3. DTA curves of gibbsite: (curve a) well crystallized sample; (curve b) poorly crystallized sample.

It is observed that the temperature and temperature range of the peak is also an indication of the degree of crystallinity: the greater the temperature, temperature range and size of the peak, the greater the degree of crystallinity.

The reason for this is that structural water is more strongly bonded in more crystalline gibbsite than in poorly crystallized samples. Therefore more energy is needed to break the bonds holding the structural water in the structure and, consequently, the temperature range and size of the peak will be relatively greater for gibbsite with a high degree of crystallinity (Table 2).

A possible explanation for the thermal transformation of gibbsite can be proposed along the lines put toward by Taylor [17]; the gibbsite structure consists of layers of hydroxyl ions (OH^-) with the sequence - - -AB · BA- - -, with interstitial aluminium ions in the octahedral holes within the closed packet layers. When such a structure is heated, there is a removal of protons from the OH^- (donor region) which consists of the anion framework of the lattice, and a transfer of the removed proton from one site to

TABLE 2

DTA results

Sample	Temperature range (°C)	Temperature of the maximum (°C)	Size of peak (cm)
Well crystallized	250–490	360	17.2
Poorly crystallized	250–430	330	7.8

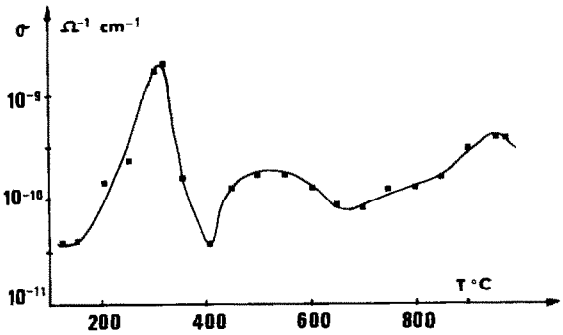

Fig. 4. Plot of electrical conductivity (σ) versus temperature of well crystallized gibbsite.

another (acceptor region). The protons combine with OH^- to form water molecules (H_2O) which are expelled from the lattice. The Al^{3+} ions migrate locally, thereby balancing the induced charge created by the removal of protons.

Electrical behaviour during dehydration

Correlation between the thermal reaction process and the degree of crystallinity was further confirmed by the electrical conductivity measurement (Figs. 4 and 5). It is clear that the electrical conductivity value at room temperature of well crystallized samples is less that that of poorly crystallized ones. Moreover, the value at the transition temperature changes appreciably in both types of samples.

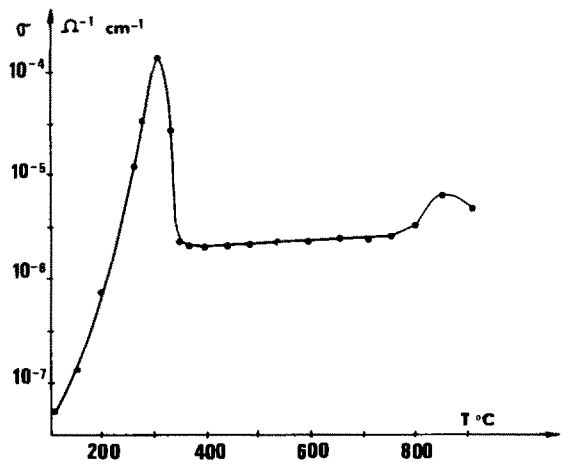

Fig. 5. Plot of electrical conductivity (σ) versus temperature of poorly crystallized gibbsite.

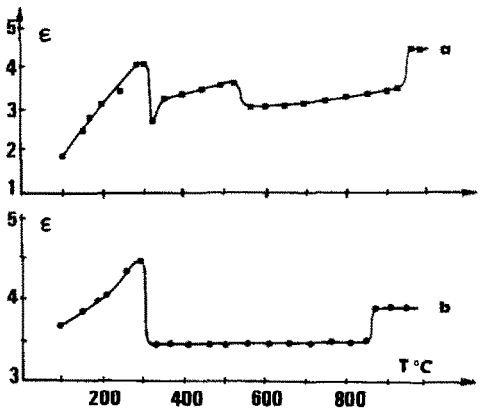

Fig. 6. Plot of dielectric constant (ε) against temperature: (curve a) well crystallized sample; (curve b) poorly crystallized sample.

The decrease in conductivity from 25°C to 100°C corresponds to the desorption of adsorbed water on the sample. The conductivity maximum at about 300°C can be ascribed to the appearance of transistory adsorbed free water vapour formed during the dehydration reaction, as occurs with many other hydrates e.g. calcium sulphate dihydrate [18,19], copper sulphate pentahydrate [20] and barium chloride dihydrate [20]. The greater increase in conductivity at 300°C, observed with poorly crystallized sample, may be due to the high specific surface area of the solid, and, therefore, to an increase in the quantity of transitory adsorbed free water vapour on the solid surface during the dehydration reaction. The second maximum at about 400°C for well crystallized sample corresponds to the dehydration of boehmite.

The dielectric constant of well crystallized gibbsite first increases on heating up to about 300°C (Fig. 6, curve a), thus revealing that an increasing number of polar water molecules are being reoriented and forced to contribute to the polarization. After having reached the peak, the dielectric constant begins to decrease on further heating as the liberated water is expelled. The presence of a maximum in the curve of variation of the dielectric constant versus temperature can be interpreted as for the electrical conductivity results (transitory adsorption of free water formed during dehydration reaction).

In poorly crystallized samples (Fig. 6, curve b), the dielectric constant value at 100°C is high compared with well crystallized samples, which shows that water is more abundant in the former owing to its fine crystallite size and greater specific surface area.

Transitory formation of boehmite

A possible explanation for the two ways in which gibbsite transforms [21] can be suggested. In the presence of water vapour, gibbsite transforms to

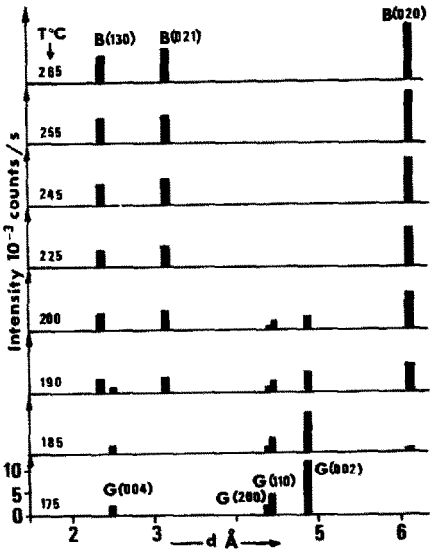

Fig. 7. Change in the intensities of some of the basal spacings of boehmite (B) and of well crystallized gibbsite (G) with the increase in temperature of the hydrothermal treatment.

boehmite, while the absence of local hydrothermal conditions causes the gibbsite to transform to χ-Al_2O_3. It can be considered that the outer periphery of the large crystallites transforms to χ-Al_2O_3 (at 300°C) and this χ-Al_2O_3 builds up a hydrothermal atmosphere inside the crystallite, thus causing the core inside to transform to boehmite. In poorly crystallized samples, the crystallite size is so small that an inside core does not exist, so that only χ-Al_2O_3 transformation takes place at 300°C.

The phase transformation of gibbsite under hydrothermal conditons up to a temperature of 265°C has confirmed the formation of boehmite: X-ray diffraction analysis shows that the intensity of the (002) line of gibbsite (Fig. 7) goes on decreasing, whereas the intensity of the strongest reflection of boehmite (020) goes on increasing with respect to temperature, and attains a maximum value after treatment at 265°C, the transformation of gibbsite to boehmite starting at 190°C. Thus, a hydrothermal atmosphere leads to transformation to boehmite only.

Actiation energy of the dehydration

The apparent activation energy of the dehydration of both types of gibbsite samples was obtained from TG and DTA investigations, using the methods of Coats and Redfern [22], Kissinger [23], Piloyan et al. [24], and Borchardt and Daniels [25]. Results show that for materials with low crystallinity, transforming directly to χ-alumina, the average value of the apparent activation energy ($E \approx 125$ kJ mol^{-1}) is relatively larger than the

value ($E \approx 73$ kJ mol^{-1}) obtained with well crystallized samples. This is in contrast with other examples given in the literature, e.g. the dehydroxylation of kaolinite for which the higher the crystallinity, the higher the value of the activation energy [26]. However, an explanation can be given based on the previous observation of Quinn and Frost [27] concerning the crystallite size: the larger activation energy value of small crystallites may be because such crystallites store energy in the form of internal disorder. When such crystallites are heated at 300°C, the product formed (χ-alumina) is almost amorphous and the activation energy of this phase is high. Similar behaviour has been reported for the dehydration of copper sulphate monohydrate [27].

Orientation relationships during the phase transformation

As discussed in the introduction, many authors consider that the gibbsite (or boehmite) → α-alumina sequence results from topotaxy and pseudomorphosis. From the X-ray analysis, it has been found that reflections corresponding to an interplanar spacing of 0.139 nm are present on all structural transformations of both well and poorly crystallized materials. Because of the persistence of this reflection, it is natural to conjecture that gibbsite possesses orientation relationships with the crystal structures formed during the thermal transformations.

Lattice dimensions of the various modifications of the crystal structure have been calculated [28] from the X-ray powder diffractograms of different phases (boehmite, χ-, γ- and α-alumina) and are given in Table 3.

Phase change in well crystallized samples (Fig. 8)

At 300°C, boehmite is formed. The cell dimension of gibbsite with $a = 0.8624$ nm is reduced to 1/3 of its value in boehmite ($a = 0.287$ nm). On heating further to 550°C, γ-Al_2O_3 is formed and the [100] of boehmite becomes the [110] axis of γ-Al_2O_3. Heating further to 1150°C, the γ-Al_2O_3 structure, having cubic symmetry, arranges itself to α-Al_2O_3 which has

TABLE 3

Lattice constants of the different phases

Phase	Lattice constants (nm)			
	a	*b*	*c*	*β*
Gibbsite (monocl)	0.8624	0.506	0.970	93° 34′
Boehmite (orthor)	0.28679	1.2219	0.37024	
γ-Al_2O_3 (cubic)	0.78072	–	–	
χ-Al_2O_3 (hex)	0.55978		0.86091	
α-Al_2O_3 (hex)	0.4759	–	1.30143	

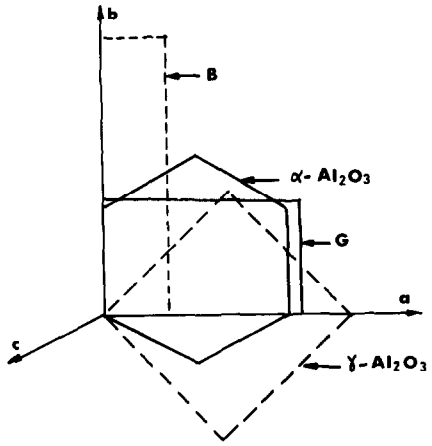

Fig. 8. Schematic representation of orientation relationships of well crystallized gibbsite in the (*a*,*b*) plane (G, gibbsite; B, boehmite).

hexagonal close-packing of oxygen atoms. Thus, the [110] of γ-Al_2O_3 changes to [21$\bar{3}$0] of α-Al_2O_3.

Phase change in poorly crystallized samples

It is seen from Fig. 9 that the [100] axis of gibbsite becomes the [01$\bar{1}$0] axis of χ-Al_2O_3. The [01$\bar{1}$0] axis of χ-Al_2O_3 at 1150°C changes to [21$\bar{3}$0] of α-Al_2O_3. The [100] axis of gibbsite is 3×0.287 nm; the [01$\bar{1}$0] of χ-alumina is 2×0.2798 nm; the [21$\bar{3}$0] of α-alumina is 3×0.2747. On the basis of the persistence of the 0.139 nm reflection in all the phases, it may be conjectured that 1/3 of the value of the '*a*' axis of gibbsite is almost equal to 2 times the [01$\bar{1}$0] of χ-alumina and three times the [21$\bar{3}$0] of α-alumina.

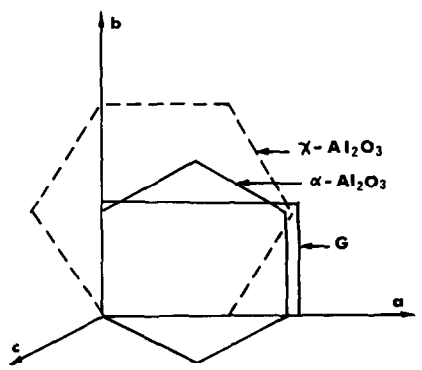

Fig. 9. Schematic representation of orientation relationships of poorly crystallized gibbsite in the (*a*, *b*) plane (G, gibbsite).

Consequently, according to the crystallinity of gibbsite, the following orientation relationship can be proposed for well crystallized (a) and poorly crystallized samples (b):

$$\text{Gibbsite}_{[100]} \rightarrow \begin{cases} \xrightarrow{(a)} \text{Boehmite}_{[100]} \rightarrow \gamma\text{-}Al_2O_3{}_{[110]} \\ \xrightarrow{(b)} \chi\text{-}Al_2O_3{}_{[01\bar{1}0]} \rightarrow \kappa\text{-}Al_2O_3{}_{[01\bar{1}0]} \end{cases} \rightarrow \alpha\text{-}Al_2O_3{}_{[21\bar{3}0]}$$

CONCLUSIONS

From the study of the thermal reactions of gibbsite, the following conclusions can be drawn:

1. The crystallinity of gibbsite governs the thermal reaction.
2. Samples with a low degree of crystallinity revealed a higher electrical conductivity than that of those with a higher degree of crystallinity. Similarly, the dielectric constant value is also a measure of the degree of crystallinity. Moreover, the changes in the values of dielectric constant and electrical conductivity with respect to temperature are readily explained on the basis of thermal transformation.
3. There are orientation relationships between the different structural modifications of alumina formed during thermal transformation.

REFERENCES

1 I. Valcton, Bauxites, Elsevier, Amsterdam, 1972.
2 J. Scott, in Extractive Metallurgy of Aluminium, Vol. I, Interscience, New York, 1963, p. 203.
3 H. Thibon, J. Charrrier and R. Tertian, Bull. Soc. Chim. Fr., 18 (1951) 384.
4 D. Papee, J. Charrier, R. Tertian and R. Houssemaine, Congrès de l'Aluminium, Paris, 1954, p. 1.
5 Y. Trambouze, in P. Pascal (Ed.), Nouveau Traité de Chimie Minérale, Vol. VI, Masson, Paris, 1961, p. 574.
6 W.H. Gitzen (Ed.), Alumina as a Ceramic Material, The American Ceramic Society, Columbus, OH, 1970, p. 17.
7 L.D. Hart (Ed.), Alumina Chemicals: Science and Technology Handbook, The American Ceramic Society, Werterville, Ohio, 1990, p. 19.
8 P. Burtin, J.P. Brunelle, M. Pijolat and M. Soustelle, Appl. Catal., 34 (1987) 225.
9 P. Burtin, J.P. Brunelle, M. Pijolat and M. Soustelle, Appl. Catal., 34 (1987) 239.
10 P. Burtin, Thesis, Université de Saint-Etienne, France, 1985.
11 G. Ervin and E.F. Osborn, J. Geol., 59 (1951) 381.
12 G. Varhegyi, J. Fekete and M. Gemesi, in Sedal (Ed.), 3rd Int. ICSOBA Congress, Nice, France, 1973, p. 575.
13 R. Schoen and E. Roberson, Am. Mineral., 55 (1970) 43.
14 K. Kal and D.R. Pahwa, Rev. Sci. Instrum., 10 (1971) 204.
15 J.K. Vij and K.K. Srivastava, Ind. J. Pure Appl. Phys., 7 (1969) 394.

16 K.S. Mazdiyanni and L.M. Brown, J. Am. Ceram. Soc., 54 (1971) 539.
17 H.F.W. Taylor, Clay Miner. Bull., 6 (1962) 45.
18 C. Eyraud, M. Murat and P. Barriac, Bull. Soc. Chim. Fr., 10 (1967) 3730.
19 M. Murat and P. Barriac, Bull. Soc. Chim. Fr., 8 (1969) 2644.
20 W.W. Wendlandt, Thermochim. Acta, 1 (1970) 11.
21 B.C. Lippens and J.H. de Boer, Acta Crystallogr., 17 (1964) 1312.
22 A.W. Coats and J.P. Redfern, Nature, 201 (1964) 68.
23 H.E. Kissinger, J. Res. Natl. Bur. Stand., 57 (1956) 217.
24 G.O. Piloyan, I.O. Ryabchikov and D.S. Novikova, Nature (London), (1960) 1229.
25 J.H. Borchardt and F. Daniels, J. Am. Chem. Soc., 79 (1957) 41.
26 J.G. Cabrera and M. Eddleston, Thermochim. Acta, 70 (1983) 237.
27 M. Quinn and M. Frost, Can. J. Chem., 33 (1955) 286.
28 A. Taylor and R.W. Floyd, Acta Crystallogr., 3 (1950) 285.